JACS
JOURNAL OF THE AMERICAN CHEMICAL SOCIETY
Communication
pubs.acs.org/JACS

The Hydroxyl Radical is a Critical Intermediate in the Voltammetric Detection of Hydrogen Peroxide

James G. Roberts, Maxim A. Voinov, Andreas C. Schmidt, Tatyana I. Smirnova, and Leslie A. Sombers*

Department of Chemistry, North Carolina State University, Raleigh, North Carolina 27695, United States

Supporting Information

ABSTRACT: Cyclic voltammetry is a widely used and powerful tool for sensitively and selectively measuring hydrogen peroxide (H_2O_2). Herein, voltammetry was combined with electron paramagnetic resonance spectroscopy to identify and define the role of an oxygen-centered radical liberated during the oxidation of H_2O_2. The spin-trap reagents, 5,5-dimethyl-1-pyrroline *N*-oxide (DMPO) and 2-ethoxycarbonyl-2-methyl-3,4-dihydro-2*H*-pyrrole-1-oxide (EMPO), were employed. Spectra exhibit distinct hyperfine patterns that clearly identify the DMPO•−OH and EMPO•−OH adducts. Multiple linear regression analysis of voltammograms demonstrated that the hydroxyl radical is a principal contributor to the voltammetry of H_2O_2, as signal is attenuated when this species is trapped. These data incorporate a missing, fundamental element to our knowledge of the mechanisms that underlie H_2O_2 electrochemistry.

The electrochemical detection of hydrogen peroxide (H_2O_2) has drawn much attention over several decades because it plays a key role in powerful analytical tools. Most notably, H_2O_2 electrochemistry underlies the performance of peroxidase-based biosensors, and thus it is of significant interest to scientists developing technologies for rapid molecular monitoring. Despite a staggering number of publications on biosensor design, the market is still far from meeting many key end-user needs. This is largely attributed to issues in stability, sensitivity, and accuracy that hinge on the selective and reliable detection of H_2O_2 at enzyme-modified electrode surfaces. Even though there is wide interest in exploiting this electrochemistry, the precise mechanisms that describe H_2O_2 redox activity at various electrode surfaces are not well understood. Electrochemical oxidation of H_2O_2 results in the generation of 2 protons, 2 electrons, and oxygen gas.

$$H_2O_2 \rightleftharpoons 2H^+ + 2e^- + O_2$$

However, this reaction is convoluted by its dependency on the electrode surface, applied potential, electrolyte composition, etc.[1] Studies have demonstrated that H_2O_2 oxidation occurs in the potential region corresponding to oxide film formation,[2] and it is favored on an oxidized platinum surface.[3] Thus, a longstanding question is how the oxidized electrode surface influences chemical reactivity. In this work, we use electron paramagnetic resonance (EPR) spectroscopy to identify the hydroxyl radical as a key intermediate species underlying the voltammetric detection of H_2O_2 at both platinum and carbon-fiber electrodes. The unexpected data advance our understanding of chemical processes occurring at the electrode surface and promise further exploitation of H_2O_2 electrochemistry in numerous applications.

Figure 1A–B depicts cyclic voltammograms for 100 mM H_2O_2 collected using a scan rate of 1 V·s^{-1} on a carbon-fiber and platinum microelectrode, respectively. Current density is plotted on the *y*-axis in order to facilitate a direct comparison. Distinct responses are observed, where anodic current is generated on platinum at a lower potential relative to carbon. We have found that fast-scan cyclic voltammetry (FSCV) is particularly useful for monitoring rapid fluctuations of biological H_2O_2 in live tissue, as it enables real-time measurements when coupled with carbon-fiber microelectrodes.[4] Thus, carbon and platinum electrode materials were also compared using a scan rate of 400 V·s^{-1} (Figure 1C–D). On carbon, peak current increased as the positive wavelimit was increased. However, the opposite trend was observed using the platinum electrode, suggesting a critical dependence on the oxidation state of the platinum surface. Oxides accumulate on platinum surfaces upon strong anodic polarization, and these can shift the potential in the positive direction during the descending sweep.[2] The atypical location of the peak at high scan rates (evident on the reverse scan) is an advantageous consequence of data filtering

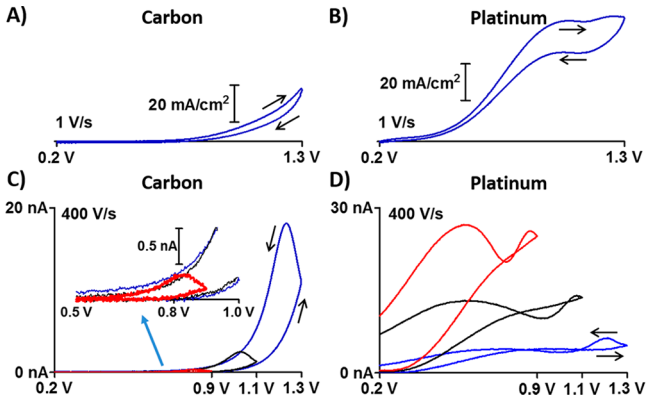

Figure 1. Representative voltammograms for 100 mM H_2O_2 on (A) carbon and (B) platinum electrodes using a scan rate of 1 V·s^{-1}. Using background subtracted FSCV at 400 V·s^{-1}, the effects of varying the positive limit are shown for (C) 200 μM H_2O_2 on carbon and (D) 20 μM H_2O_2 on platinum.

Received: December 22, 2015
Published: February 3, 2016

DOI: 10.1021/jacs.5b13376
J. Am. Chem. Soc. 2016, 138, 2516–2519

(Figure S1),[5] resulting in a predictable and well-resolved signal that allows rapid qualitative identification and accurate quantitation. Additional differences between these materials are evident when investigating the effects of scan rate (Figure S2).

EPR spectroscopy was used to investigate if short-lived radical species are generated in H_2O_2 oxidation. Two spin traps, 2-ethoxycarbonyl-2-methyl-3,4-dihydro-2*H*-pyrrole-1-oxide (EMPO) and 5,5-dimethyl-1-pyrroline *N*-oxide (DMPO), were added to the H_2O_2 solution in separate experiments. The spin trap itself remains EPR silent until adduct formation. Figure 2 illustrates reaction paths for two possible oxygen-centered radicals with EMPO and DMPO and their respective spectra.

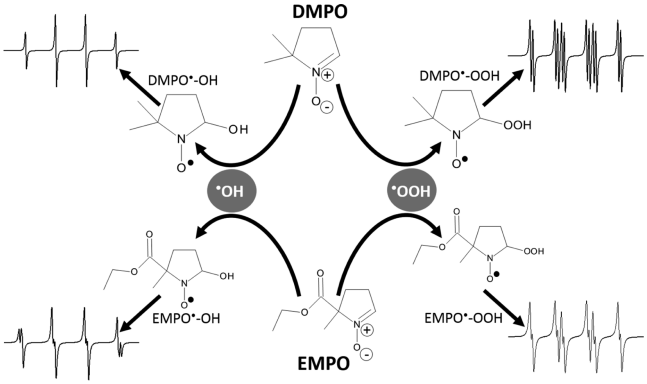

Figure 2. Suspected trap adducts with respective spectra.

The left path shows hydroxyl radical addition to the α carbon of the spin traps, while the right path illustrates the trapping of a superoxide radical. The resulting spectra demonstrate the qualitative power of EPR spectroscopy. A platinum microelectrode was lowered into a 200 μL electrochemical cell with a Ag/AgCl reference electrode, and a traditional cyclic waveform was continuously applied for 30 min (+0.2 to +1.3 V, 1 V·s^{-1}). Continuous wave X-band EPR spectra collected for samples that contained both 5 mM H_2O_2 and 5 mM EMPO show a clear four-line 1:2:2:1 splitting pattern characteristic of the EMPO$^{\bullet}$−OH adduct (Figure 3A). The experimental EPR spectra were least-squares simulated using a Voigt function with previously described software[12,13] to yield Species 1: A_N = 14.11 ± 0.02 G, A_H = 15.00 ± 0.04 G, and A_H = 0.82 ± 0.03 G; Species 2: A_N = 14.02 ± 0.03 G and A_H = 12.62 ± 0.02 G.[6] Literature values for the EMPO$^{\bullet}$−OH adduct are Species 1: A_N = 14.0 G, A_H = 15.1 G, and A_H = 0.9 G; Species 2: A_N = 14.0 G and A_H = 12.7 G.[7] By contrast, samples that contained only EMPO (no H_2O_2) resulted in spectra that did not exhibit any discernible signal above noise (Figure 3B). The EPR spin trapping experiments are known to produce adduct artifacts, and it can be contended that hydroperoxide radical adducts can rapidly decay to hydroxyl radical adducts, resulting in false identification of the principal radical.[8] However, EMPO is the most efficient spin trap for the detection of oxygen-centered free radicals. The EMPO$^{\bullet}$−OOH adduct is about five times more stable than the corresponding DMPO adduct, and it does not readily decay to EMPO$^{\bullet}$−OH, making the experimental data less ambiguous.[9] No signal characteristic of the EMPO$^{\bullet}$−OOH adduct was detected in our experiments, allowing us to conclude that the decomposition of the DMPO$^{\bullet}$−OOH adduct is not a source of the observed DMPO$^{\bullet}$−OH adduct (Figure 3C). Additional experiments were carried out using a fast cyclic

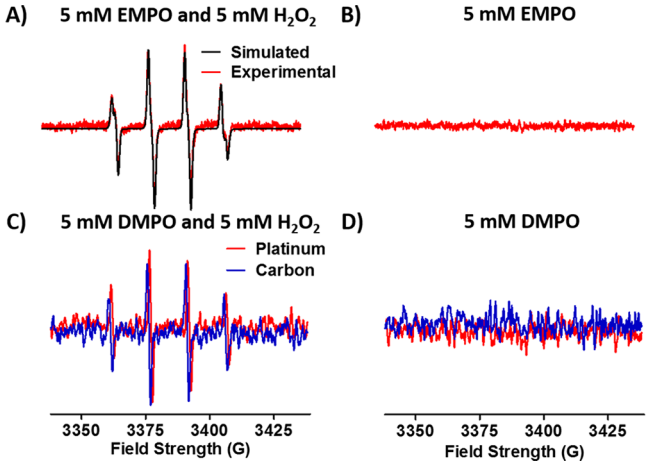

Figure 3. EPR spectra implicate the hydroxyl radical in the electrochemical oxidation of H_2O_2. (A) Platinum electrodes cycled (1 V·s^{-1}) in the presence of EMPO and H_2O_2 generated spectra (red) consistent the simulated spectrum (black). (B) EMPO spectrum in the absence of H_2O_2. (C) Spectra generated using carbon (blue) or platinum (red) electrodes (400 V·s^{-1}) for DMPO in the presence and (D) absence of H_2O_2.

waveform (+0.2 to +1.3 V, 400 V·s^{-1}, 100 Hz) at both carbon fiber and platinum microelectrodes. The resulting spectra again show a clear hyperfine splitting pattern characteristic of the hydroxyl radical adduct with no evidence of the hydroperoxide adduct (Figure 3C−D). The hyperfine coupling constants fitted for these data are presented in Table S-1. It is important to note that the absence of an EPR signal for a specific radical species does not prove that it is not transiently formed. Dimethyl sulfoxide (DMSO, 20-fold excess) was added to the solution to selectively scavenge hydroxyl radicals.[10] The typical four-line spectrum was abolished (Figure S3). As DMSO quenching of the hydroxyl radical generates a methyl radical, the characteristic six-line spectrum for a DMPO$^{\bullet}$−CH_3 adduct was also expected, but not observed. However, the absence of the methyl adduct does not exclude hydroxyl radical quenching by DMSO. Indeed, similar observations have been reported by others, although under different experimental conditions.[11]

Experiments were designed to assess the possibility that the radicals originated at a location other than the working electrode. To investigate the reference electrode, a microagar salt bridge was constructed.[12] This enabled stable potentials and effectively excluded the Ag/AgCl reference electrode from the sample. The resulting spectra were identical to those generated using the direct-contact reference (data not shown), verifying that the site of radical formation was not the reference electrode. An oxygen-centered radical could also originate from the supporting electrolyte. Trizma buffer and phosphate buffered saline were compared to uncover any contribution from Trizma (which possesses three terminal hydroxyl groups) on adduct formation, and equivalent spectra resulted for both (data not shown). Additional control experiments included holding the potential (+0.2 V) without cycling, or allowing the potential of the electrode to float in a solution of H_2O_2 and DMPO. The collected spectra resulted in no observable signal (data not shown). To the best of our knowledge this report is the first direct demonstration of hydroxyl radical production in the anodic decomposition of H_2O_2. The radical was generated at both platinum and carbon electrodes, using a wide range of scan rates, only in the presence of H_2O_2. The hydroperoxide

DOI: 10.1021/jacs.5b13376
J. Am. Chem. Soc. 2016, 138, 2516−2519

radical was not observed. Hall et al. have proposed that H_2O_2 reduces surface oxides, and the observed current is generated in the reoxidation of platinum.[1b]

$$Pt(OH)_2 + H_2O_2 \rightleftharpoons Pt(OH)_2 \cdot H_2O_2$$

$$Pt(OH)_2 \cdot H_2O_2 \rightleftharpoons Pt^0 + 2H_2O + O_2$$

Far less is known about the oxidation of H_2O_2 on carbon. This process is pH dependent (Figure S4), demonstrating that H^+ or OH^- ions take part in the electrode reaction. For example, the hydroxyl radical might be generated from H_2O_2 as follows:[13]

$$H_2O_2 + H^+ + e^- \rightarrow OH^{\cdot} + H_2O \quad E^o = 1.14\ \text{V vs NHE}$$

The free energy change for the dissociation of H_2O_2 into 2 hydroxyl radicals is ~50 kcal (~1.1 V vs NHE), and the conversion of radicals into OH^- ions occurs readily.[14] Thus, it is energetically feasible that a hydroxyl radical intermediate is generated in the decomposition of H_2O_2. Reaction could then take place between a free hydroxyl radical and oxygen-containing groups on the oxidized carbon surface, for example:

$$CO\cdots OH + OH^{\bullet} \rightleftharpoons C^0 + O_2 + H_2O$$

with current generated in the reoxidation of carbon.

$$C^0 + 2H_2O - 4e^- \rightleftharpoons CO_2 + 4H^+$$

However, at present these mechanisms are speculative.

Adenosine[15] and histamine[16] are other neurochemicals that generate an unusual fast-scan voltammetric signature in which peak current is evident on the reverse scan at approximately +1.2 V when using a similar waveform (Figure 4). In order to determine if a peak in this position is generally indicative of a radical intermediate, the trapping experiment was replicated using 5–10 mM adenosine or 5 mM histamine in solution with 5 mM DMPO, an efficient trap of both nitrogen- and carbon-centered radicals. The adenosine concentration was increased to nearly the solubility limit, to account for the possibility that an adenosine–DMPO adduct may have additional hyperfine splitting resulting in reduced signal intensity.[17] Despite this, the EPR spectra did not exhibit a significant signal over the noise (data not shown). Although this does not absolutely exclude the possibility of radical generation during voltammetry of these molecules, the results suggest that, despite similar voltammograms, hydroxyl radical formation is specific to the oxidation of H_2O_2.

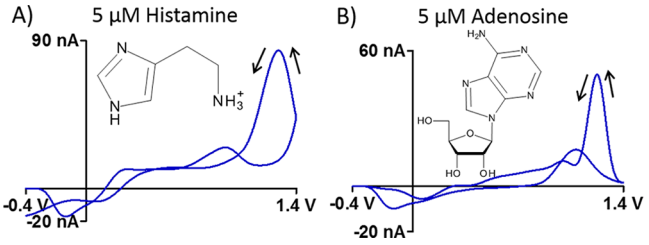

Figure 4. Representative voltammograms for (A) histamine and (B) adenosine collected on carbon-fiber microelectrodes.

Activated metal surfaces catalyze the disproportionation of H_2O_2 such that bubbles of oxygen form on gold, for example, when exposed to H_2O_2 solution. Continuously scanning the electrode serves to activate the surface, and this alone may induce disproportionation of H_2O_2 and generation of the hydroxyl radical. Thus, experiments were conducted to confirm that it is the electrochemical oxidation of H_2O_2 that generates hydroxyl radicals. Using carbon-fiber microelectrodes, voltammograms for H_2O_2 were collected in the presence and absence of DMPO in 10-fold excess (Figure 5). DMSO was also tested, at 100-fold excess.[18] The voltammograms of the spin-trap reagents demonstrate some current (left panels) that is evident in samples containing both the trap and H_2O_2 (right panels). Importantly, currents generated for samples containing multiple electroactive species should be additive, such that the sum of the voltammograms for each analyte comprises the voltammogram for the mixed sample.[19] Current is attenuated, however, if there is a chemical reaction that partially consumes analytes. In these experiments, a summation of current was generally observed, except at +1.2 V where the oxidation of H_2O_2 is apparent. At this potential, the sum of the currents for the individual analytes exceeds the current observed for the mixture. Since all individual analytes generated predictable currents that increased linearly with respect to concentration, multiple linear regression (MLR) was used to solve for the concentration of H_2O_2 in each mixture,[20] following the equations:

$$\alpha\cdot(\text{TrapCV}) + \beta\cdot(H_2O_2\text{CV}) = (\text{MixCV}) \quad (1)$$

$$\frac{\beta}{\delta}\cdot(H_2O_2\text{CV}) = [H_2O_2]_{H_2O_2\text{CV}} \quad (2)$$

$$\frac{\beta}{\delta} = [H_2O_2]_{\text{MixCV}} \quad (3)$$

where TrapCV and H_2O_2CV are normalized voltammograms for each analyte, MixCV is a voltammogram for the mixed analyte solution, α and β are coefficients with units of nA, and δ is a calibration factor for each electrode describing sensitivity to H_2O_2 (nA·μM^{-1}). The results are presented in Figure 5C–D and listed in Table S-2. The concentration of H_2O_2 in both the DMPO–H_2O_2 mixture and the DMSO–H_2O_2 mixture is significantly less than that measured in samples containing the same concentration of H_2O_2 alone. This suggests that the voltammetric detection of H_2O_2 directly involves the hydroxyl radical, at both carbon and platinum electrodes. However, it is also possible that the spin trapping reagents reduced electrode sensitivity (fouling). To investigate this, a parallel experiment was performed using 1 μM histamine and 1 mM DMPO. Histamine was chosen because its voltammogram exhibits peak current at a comparable potential to that of H_2O_2 (Figure 4). MLR predicted equal concentrations of histamine in solutions of histamine and mixed solutions of histamine and DMPO (Table S-3). Thus, electrode sensitivity is not significantly attenuated by spin trap exposure, and the hydroxyl radical plays a fundamental role in the voltammetric detection of H_2O_2.

Overall, these results identify the hydroxyl radical as a key species underlying oxidation of H_2O_2 at both carbon and platinum electrode substrates. The direct detection of this chemical intermediate is significant due to broad interest in H_2O_2 electrochemistry to serve a variety of purposes, and it promises to inform continued innovation in biosensor development for a range of diagnostic applications across diverse scientific disciplines.

DOI: 10.1021/jacs.5b13376
J. Am. Chem. Soc. 2016, 138, 2516–2519

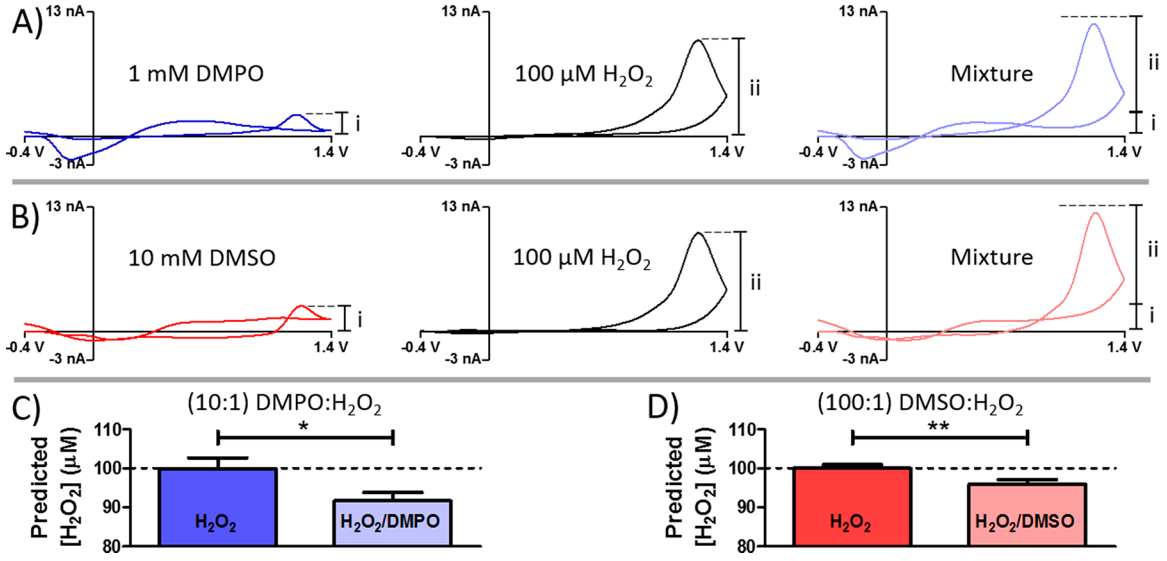

Figure 5. Electrochemical signal is hydroxyl radical dependent. (A, B) Representative voltammograms (carbon electrodes) for H_2O_2, spin trap reagents, and mixtures of the two. (C, D) Incorporation of a spin trap reagent significantly attenuated the signal evident in the electrochemical oxidation of H_2O_2 (Student's *t* test, $p = 0.0150$ and 0.0057, respectively, $n = 4$ electrodes).

■ ASSOCIATED CONTENT

Supporting Information

The Supporting Information is available free of charge on the ACS Publications website at DOI: 10.1021/jacs.5b13376.

Experimental details and data (PDF)

■ AUTHOR INFORMATION

Corresponding Author

*lasomber@ncsu.edu

Notes

The authors declare no competing financial interest.

■ ACKNOWLEDGMENTS

This research is supported by the National Science Foundation (CHE-1151264). EPR instrumentation was supported by grants from the National Institutes of Health (RR023614), the NSF (CHE-0840501), and NCBC (2009-IDG-1015). Thanks to Steve Feldberg (Brookhaven National Lab) for helpful discussions.

■ REFERENCES

(1) (a) Hall, S. B.; Khudaish, E. A.; Hart, A. L. *Electrochim. Acta* **1998**, *43*, 2015−2024. (b) Hall, S. B.; Khudaish, E. A.; Hart, A. L. *Electrochim. Acta* **1998**, *43*, 579−588. (c) Hall, S. B.; Khudaish, E. A.; Hart, A. L. *Electrochim. Acta* **1999**, *44*, 4573−4582.

(2) Hickling, A.; Wilson, W. H. *J. Electrochem. Soc.* **1951**, *98*, 425−433.

(3) (a) Lingane, J. J.; Lingane, P. J. *J. Electroanal. Chem.* **1963**, *5*, 411−419. (b) Muller, L. *J. Electroanal. Chem. Interfacial Electrochem.* **1968**, *16*, 531−539. (c) Lingane, J. J. *J. Electroanal. Chem.* **1961**, *2*, 296−309.

(4) (a) Sanford, A. L.; Morton, S. W.; Whitehouse, K. L.; Oara, H. M.; Lugo-Morales, L. Z.; Roberts, J. G.; Sombers, L. A. *Anal. Chem.* **2010**, *82*, 5205−10. (b) Lugo-Morales, L. Z.; Loziuk, P. L.; Corder, A. K.; Toups, J. V.; Roberts, J. G.; McCaffrey, K. A.; Sombers, L. A. *Anal. Chem.* **2013**, *85*, 8780−6. (c) Spanos, M.; Gras-Najjar, J.; Letchworth, J. M.; Sanford, A. L.; Toups, J. V.; Sombers, L. A. *ACS Chem. Neurosci.* **2013**, *4*, 782−9.

(5) Atcherley, C. W.; Vreeland, R. F.; Monroe, E. B.; Sanchez-Gomez, E.; Heien, M. L. *Anal. Chem.* **2013**, *85*, 7654−8.

(6) (a) Smirnov, A. I.; Belford, R. L. *J. Magn. Reson., Ser. A* **1995**, *113*, 65−73. (b) Smirnova, T. I.; Smirnov, A. I.; Clarkson, R. B.; Belford, R. L. *J. Phys. Chem.* **1995**, *99*, 9008−9016.

(7) Minotti, G.; Aust, S. D. *J. Biol. Chem.* **1987**, *262*, 1098−1104.

(8) (a) Finkelstein, E.; Rosen, G. M.; Rauckman, E. J. *Arch. Biochem. Biophys.* **1980**, *200*, 1−16. (b) Finkelstein, E.; Rosen, G. M.; Rauckman, E. J. *Molecular Pharmacology* **1982**, *21*, 262−5. (c) Ranguelova, K.; Mason, R. P. *Magn. Reson. Chem.* **2011**, *49*, 152−8.

(9) Olive, G.; Mercier, A.; Le Moigne, F.; Rockenbauer, A.; Tordo, P. *Free Radical Biol. Med.* **2000**, *28*, 403−408.

(10) Voinov, M. A.; Sosa Pagan, J. O.; Morrison, E.; Smirnova, T. I.; Smirnov, A. I. *J. Am. Chem. Soc.* **2011**, *133*, 35−41.

(11) (a) Eberhardt, M. K. Formation of Reactive Oxygen Metabolites in Vivo. *Reactive Oxygen Metabolites: Chemistry and Medical Consequences*; CRC Press: Boca Raton, FL, 2001; p 117. (b) Eberhardt, M. K. Chemistry of Oxygen-Derived Radicals. *Reactive Oxygen Metabolites: Chemistry and Medical Consequences*; CRC Press: Boca Raton, FL, 2001; p 70.

(12) Shao, X. M.; Feldman, J. L. *J. Neurosci. Methods* **2007**, *159*, 108−15.

(13) Bard, A. J.; Parsons, R.; Jordan, J. International Union of Pure and Applied Chemistry. *Standard Potentials in Aqueous Solution*, 1st ed.; M. Dekker: New York, 1985; p 834.

(14) (a) Bockris, J. O.; Oldfield, L. F. *Trans. Faraday Soc.* **1955**, *51*, 249−259. (b) Coms, F. D. *Ecs Transactions* **2008**, *16*, 235−255.

(15) Ross, A. E.; Venton, B. J. *Analyst* **2012**, *137*, 3045−51.

(16) (a) Chang, S. Y.; Jay, T.; Munoz, J.; Kim, I.; Lee, K. H. *Analyst* **2012**, *137*, 2158−65. (b) Pihel, K.; Hsieh, S.; Jorgenson, J. W.; Wightman, R. M. *Biochemistry* **1998**, *37*, 1046−52.

(17) Bernofsky, C.; Bandara, B. M.; Hinojosa, O.; Strauss, S. L. *Free Radical Res.* **1990**, *9*, 303−15.

(18) (a) Dixon, W. T.; Norman, R. O. C.; Buley, A. L. *J. Chem. Soc.* **1964**, 3625−3634. (b) Lagercrantz, C.; Forshult, S. *Acta Chem. Scand.* **1969**, *23*, 811−817.

(19) Bard, A. J.; Faulkner, L. R. *Electrochemical Methods: Fundamentals and Applications*, 2nd ed.; John Wiley: New York, 2001; p 833.

(20) (a) Brown, S. D.; Bear, R. S., Jr. *Crit. Rev. Anal. Chem.* **1993**, *24*, 99−131. (b) Bessant, C.; Saini, S. *J. Electroanal. Chem.* **2000**, *489*, 76−83.

DOI: 10.1021/jacs.5b13376
J. Am. Chem. Soc. 2016, 138, 2516−2519